Supporting Information for

Anthracene-based Molecular Rotor as Theranostic Agent for Viscosity Sensing and Imaging-guided Photodynamic Therapy

Ailada Jantasin[a], Supranee Watpathomsub[b], Thitima Pewklang[a], Tunyawat Khrootkaew[a], Sirimongkon Aryamueang[a], Bongkot Ouengwanarat[a], Kantapat Chansaenpak[c], Mongkol Sukwattanasinitt[d], Anyanee Kamkaew[a]*

[a]*School of Chemistry, Institute of Science, Suranaree University of Technology, Nakhon Ratchasima 30000, Thailand*

[b]*Faculty of Medicine, Bangkokthonburi University, Bangkok 10170, Thailand*

[c]*National Nanotechnology Center, National Science and Technology Development Agency, Thailand Science Park, Pathum Thani, 12120, Thailand*

[d]*Thailand Nanotec-CU Center of Excellence on Food and Agriculture, Department of Chemistry, Faculty of Science, Chulalongkorn University, Bangkok 10330, Thailand*

**E-mail: anyanee@sut.ac.th*

Contents

1. General information

All chemical reagents and solvents were used as received in high quality without further purification from TCI, Sigma-Aldrich, and Acros. The reactions were monitored by thin-layer chromatography (TLC) carried out on Merck silica gel 60 PF_{254} and visualized under a UV lamp (λ = 254, 366 nm). Column chromatography purifications were performed with Merck silica gel 60H (particle size 0.06−0.2 mm; 70−230 mesh ASTM). ^{1}H and ^{13}C nuclear magnetic resonance (NMR) were recorded using Bruker AVANCE 500 (500 MHz) in chloroform-*d*. Chemical shifts of ^{1}H-NMR and ^{13}C-NMR spectra are expressed in ppm (*δ*) relative to the internal TMS or residual non-deuterated solvent peak as internal standard. Splitting patterns for the spin multiplicity of the signals are informed as singlet (s), doublet (d), triplet (t), multiplet (m), doublet of doublet (dd), and combinations thereof. High-resolution mass spectrometry (HRMS) with electrospray Ionization (ESI) was performed in negative ion mode. The fluorescence lifetime was measured using a time-correlated single-photon counting (TCSPC) module (TimeTagger, Swabian GmbH) coupled to a single-photon-counting avalanche photodiode (SPCM-AQRH-44, Excelitas Technologies).

2. Synthetic procedures and characterization

Synthesis of 1-ethyl-2,3,3-trimethyl-*3H*-naphtho[2,3-*f*]indol-1-ium (3)

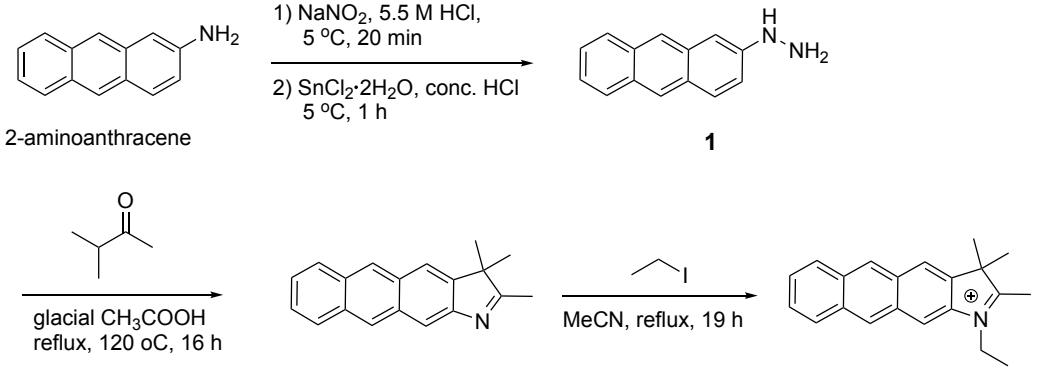

In a round bottle flask, the suspension of 2-aminoanthracene (0.7174 g, 3.712 mmol) in 5.5 M HCl (15.0 mL) was cooled at 5 °C in an ice bath. The solution of sodium nitrite (0.5272 g, 7.642 mmol) in H_2O (6.0 mL), stirring at 5 °C in the ice bath, was added dropwise with continuous stirring, then the reaction was stirred at 5 °C in the ice bath for 20 min. The cold solution of $SnCl_2{\cdot}2H_2O$ (4.1896 g, 18.567 mmol) in conc. HCl (8.0 mL) was added dropwise and stirred in the ice bath for 1 h. The reaction was neutralized with a saturated base solution. NaOH was then extracted with CH_2Cl_2. The organic layer was washed with brine, dried over $MgSO_4$, and evaporated to afford a dark brown solid (**1**), which was carried forward without further purification.

The 3-methyl-2-butanone (1.500 mL, 13.93 mmol) was added to compound **1** (0.8159 g, 3.918 mmol) in a glacial acetic acid (13.0 mL) was refluxed. After refluxing for 16 h, the glacial acetic acid was removed under reduced pressure. The residual solution was dissolved in CH_2Cl_2 and neutralized with sat. NaOH was then extracted with brine. The organic layer dried over $MgSO_4$

and was evaporated to afford a dark brown solid (**2**), which was carried forward without further purification.

The compound **2** (0.8954 g, 3.452 mmol) was dissolved in 20.0 mL of MeCN: $CHCl_3$ (3:1), followed by adding the iodoethane (1.400 mL, 17.14 mmol). The mixture was refluxed for 19 h, then cooled, and the solvent was removed under reduced pressure. After dissolving the residual solution in CH_2Cl_2, the solution was extracted with saturated NaCl. $Na_2S_2O_3$ and brine, respectively. The organic layer was dried over $MgSO_4$ and evaporated to afford a dark brown solid (**3**), which was used without further purification. (0.9621 g, 90% from 2-aminoanthracene)

Synthesis of 2-((*E*)-2-((*E*)-2-chloro-3-((*E*)-2-(1-ethyl-3,3-dimethyl-1,3-dihydro-2H-naphtho[2,3-*f*]indol-2-ylidene)ethylidene)cyclohex-1-en-1-yl)vinyl)-1-ethyl-3,3-dimethyl-3*H*-naphtho[2,3-*f*]indol-1-ium (SCy7)

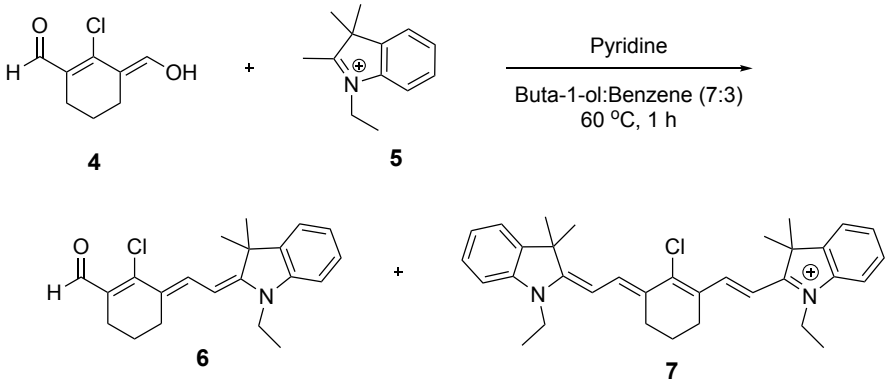

4 **5** **6** **7**

Compound **4** (0.2400 g, 1.390 mmol) was dissolved in 8.0 mL of a mixture of butan-1-ol and benzene (7:3). Compound **5** (0.4342 g, 1.382 mmol) and pyridine (0.112 mL, 1.38 mmol) were added, and the reaction was heated at 60 °C for 1 h. The solvent was removed by the evaporator, and the crude product was purified by silica chromatography eluting with MeOH: CH_2Cl_2 (0:100 to 3:97 (v/v)) to yield 0.3068 g (47%) of compound **6** as a red-orange oil product.

Synthesis of 2-((*E*)-2-((*E*)-2-chloro-3-(2-((*E*)-1-ethyl-3,3-dimethylindolin-2-ylidene) ethylidene)cyclohex-1-en-1-yl)vinyl)-1-ethyl-3,3-dimethyl-3*H*-naphtho[2,3-*f*]indol-1-ium (ASCy7)

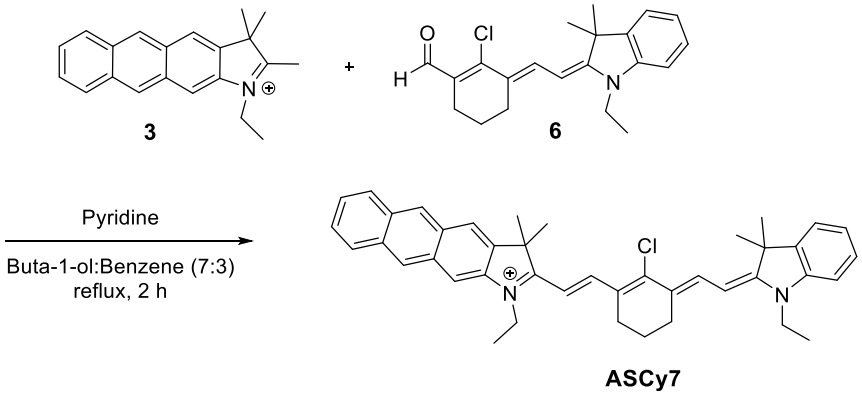

3 **6** **ASCy7**

Compound **6** (0.0771 g, 0.165 mmol) was dissolved in 3.0 mL of butan-1-ol: benzene (7:3). Compound **3** (0.0480 g, 0.166 mmol) and pyridine (0.013 mL, 0.16 mmol) were added. After refluxing for 2 h, the reaction was cooled down, and the solvent was removed under reduced pressure. The residue was purified by silica chromatography eluting with MeOH: CH_2Cl_2 (0:100 to 3:97 (v/v)) to yield 0.0407 g (33%) of compound **ASCy7** as a dark green solid product. ^{1}H NMR (500 MHz, $CDCl_3$): δ 8.61 (s, 1H), 8.53 (d, *J* = 12.1 Hz, 2H), 8.29 (d, *J* = 13.9 Hz, 1H), 8.18 – 8.11 (m, 2H), 7.99 (dd, *J* = 14.2, 8.3 Hz, 3H), 7.58 – 7.43 (m, 5H), 7.35 (t, *J* = 7.6 Hz, 2H), 7.22 – 7.17 (m, 1H), 7.07 (d, *J* = 8.3 Hz, 1H), 6.30 (d, *J* = 16.6 Hz, 1H), 6.05 (d, *J* = 13.9 Hz, 1H), 4.42 – 4.33 (m, 2H), 4.08 (q, *J* = 7.3 Hz, 2H), 2.74 (t, *J* = 6.3 Hz, 2H), 2.70 – 2.66 (m, 3H), 2.59 (s, 12H), 2.13 (s, 3H). ^{13}C NMR (125 MHz) δ 174.52, 170.48, 150.02, 144.28, 142.93, 141.74, 140.71, 138.19, 133.75, 132.37, 131.91, 130.87, 130.26, 129.16, 128.59, 128.18, 127.89, 127.31, 126.77, 125.82, 125.63, 124.68, 122.09, 120.31, 110.89, 109.92, 101.52, 99.43, 51.73, 49.48, 49.31, 49.14, 48.97, 48.80, 40.33, 39.17, 30.65, 29.47, 27.91, 27.63, 26.37, 22.46, 20.54, 13.85, 12.82. HRMS calculated for $C_{42}H_{44}ClN_2^+$ calculated: 611.3188; found 611.3185.

Synthesis of 2-((*E*)-2-((*E*)-2-chloro-3-((*E*)-2-(1-ethyl-3,3-dimethyl-1,3-dihydro-2*H*-naphtho [2,3-*f*]indol-2-ylidene)ethylidene)cyclohex-1-en-1-yl)vinyl)-1-ethyl-3,3-dimethyl-3*H*-naphtho[2,3-*f*]indol-1-ium (SCy7)

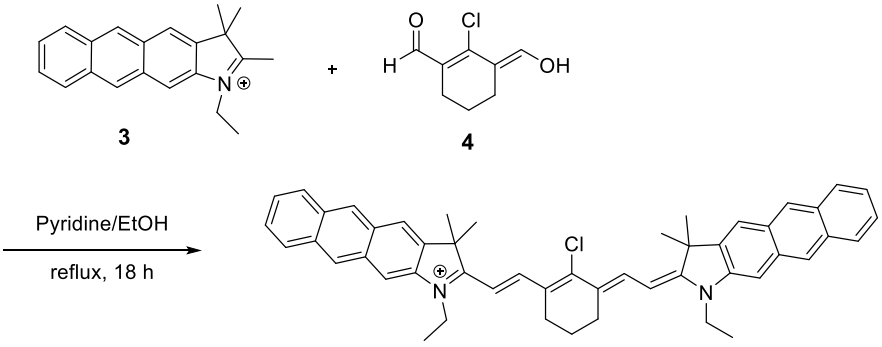

SCy7

The compound **4** (0.2060 g, 1.193 mmol) was dissolved in EtOH (8.0 mL). The compound **3** (0.9621 g, 3.336 mmol) and pyridine (0.600 mL, 7.43 mmol) were added. After refluxing for 18 h, the reaction was cooled down, and then the solvent was removed under reduced pressure. The residue was purified by silica chromatography eluting with MeOH: CH_2Cl_2 (0:100 to 3:97 (v/v)) to yield 0.0715 g (8%) of **SCy7** as a brown-green solid product. ^{1}H NMR (500 MHz, $CDCl_3$): δ 8.64 (s, 1H), 8.54 (s, 1H), 8.49 (d, *J* = 14.0 Hz, 1H), 8.14 (d, *J* = 9.0 Hz, 1H), 8.03 (d, *J* = 8.4 Hz, 1H), 7.99 (d, *J* = 8.4 Hz, 1H), 7.61 – 7.52 (m, 1H), 7.52 – 7.44 (m, 2H), 6.29 (d, *J* = 14.0 Hz, 1H), 4.40 (d, *J* = 7.2 Hz, 2H), 2.86 – 2.76 (m, 2H), 2.61 (s, 3H), 2.20 – 2.09 (m, 7H) ppm. ^{13}C NMR (125 MHz, $CDCl_3$): δ 173.4, 149.7, 143.1, 138.8, 133.2, 132.6, 132.0, 130.9, 130.4, 129.4, 128.5, 128.2, 127.7, 127.0, 126.1, 125.9, 120.4, 111.3, 101.1, 51.7, 41.1, 40.5, 28.0, 27.0, 21.0, 13.2 ppm. HRMS calculated for $C_{50}H_{48}ClN_2^+$ calculated: 711.3501; found 711.3502.

Note: The %yield of **SCy7** was low since the starting materials, which are compounds **3** and **4**, were used without purification.

3. Photophysical properties

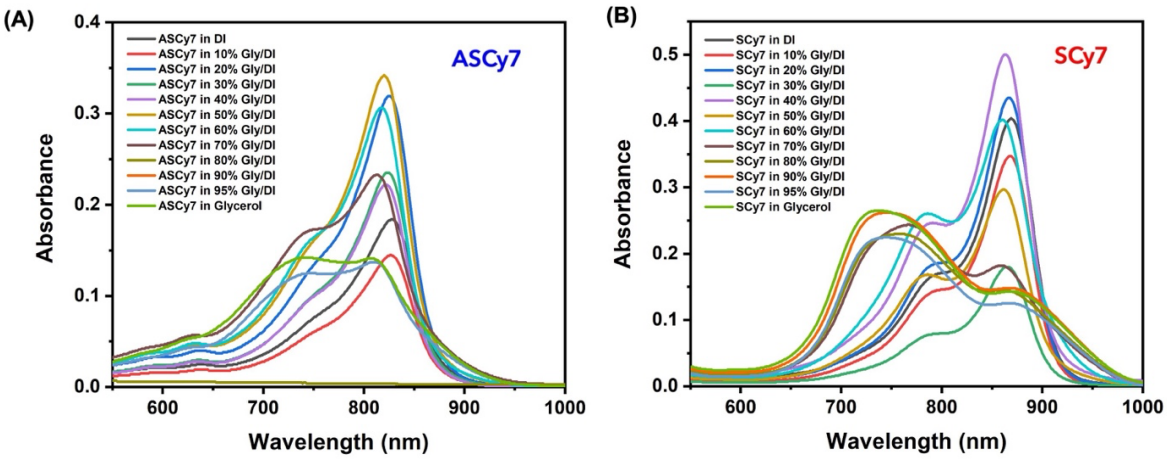

Figure S1. Absorption spectral changes of (A) **ASCy7** and (B) **SCy7** in glycerol/DI mixtures.

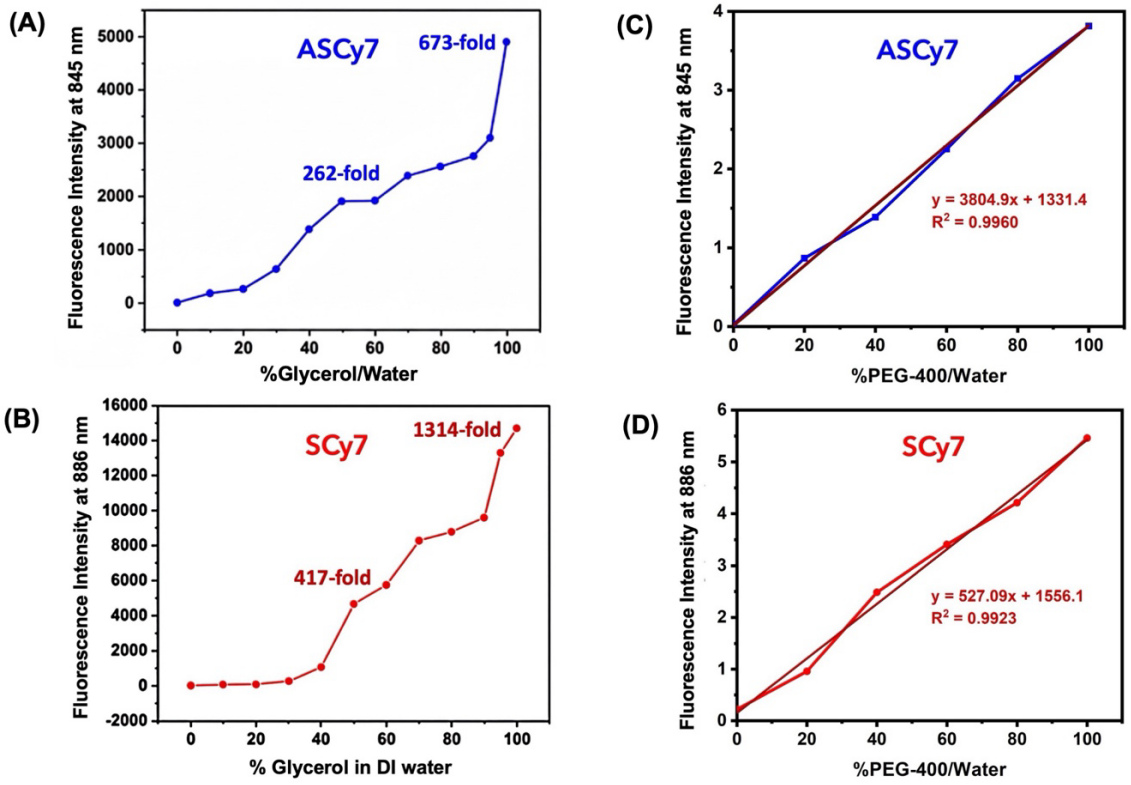

Figure S2. Relative fluorescence intensity changes of 5 μM (A) **ASCy7** in Glycerol/DI, (B) **SCy7** in Glycerol/DI, (C) **ASCy7** in PEG400/DI, (D) **SCy7** in PEG400/DI.

4. Hydrodynamic Size of ASCy7 and SCy7

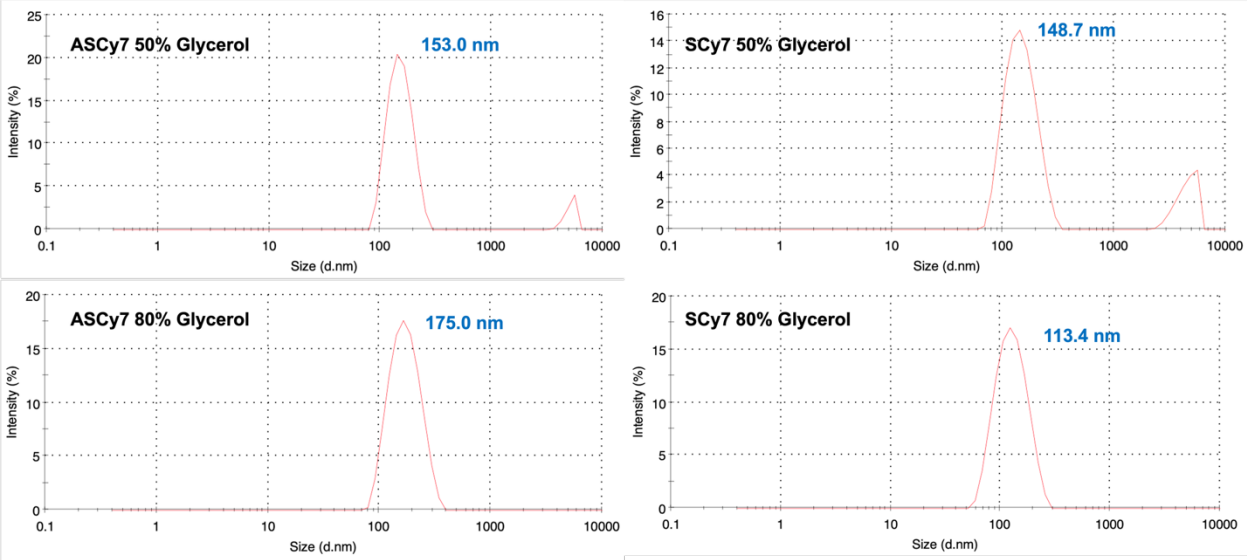

Figure S3. Hydrodynamic size measurement of **ASCy7** and **SCy7** in 50% and 80% glycerol/water systems by dynamic light scattering.

5. Fluorescence lifetime decay curve

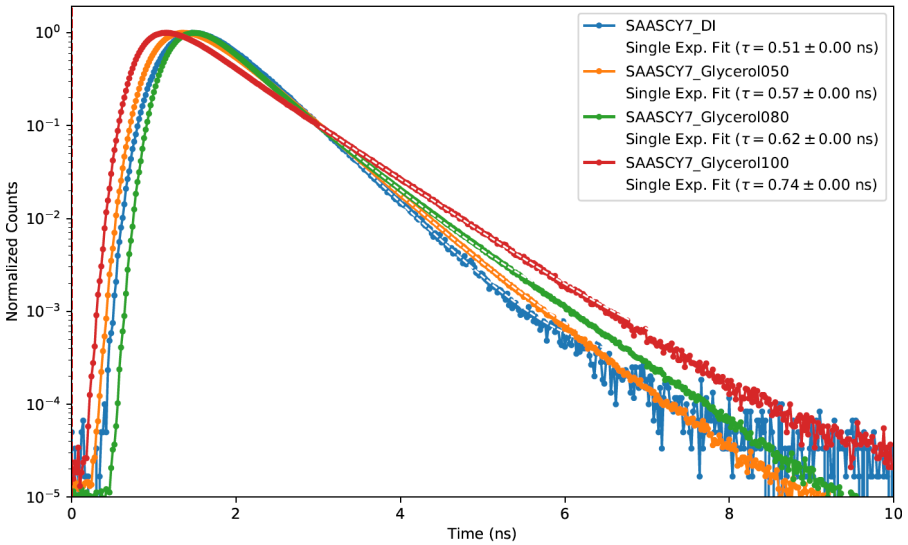

Figure S4. Fluorescence decays of **ASCy7** under different viscosity conditions.

6. Singlet oxygen ($^1O_2$) generation assay

6.1. DPBF-based assay of ASCy7 and SCy7

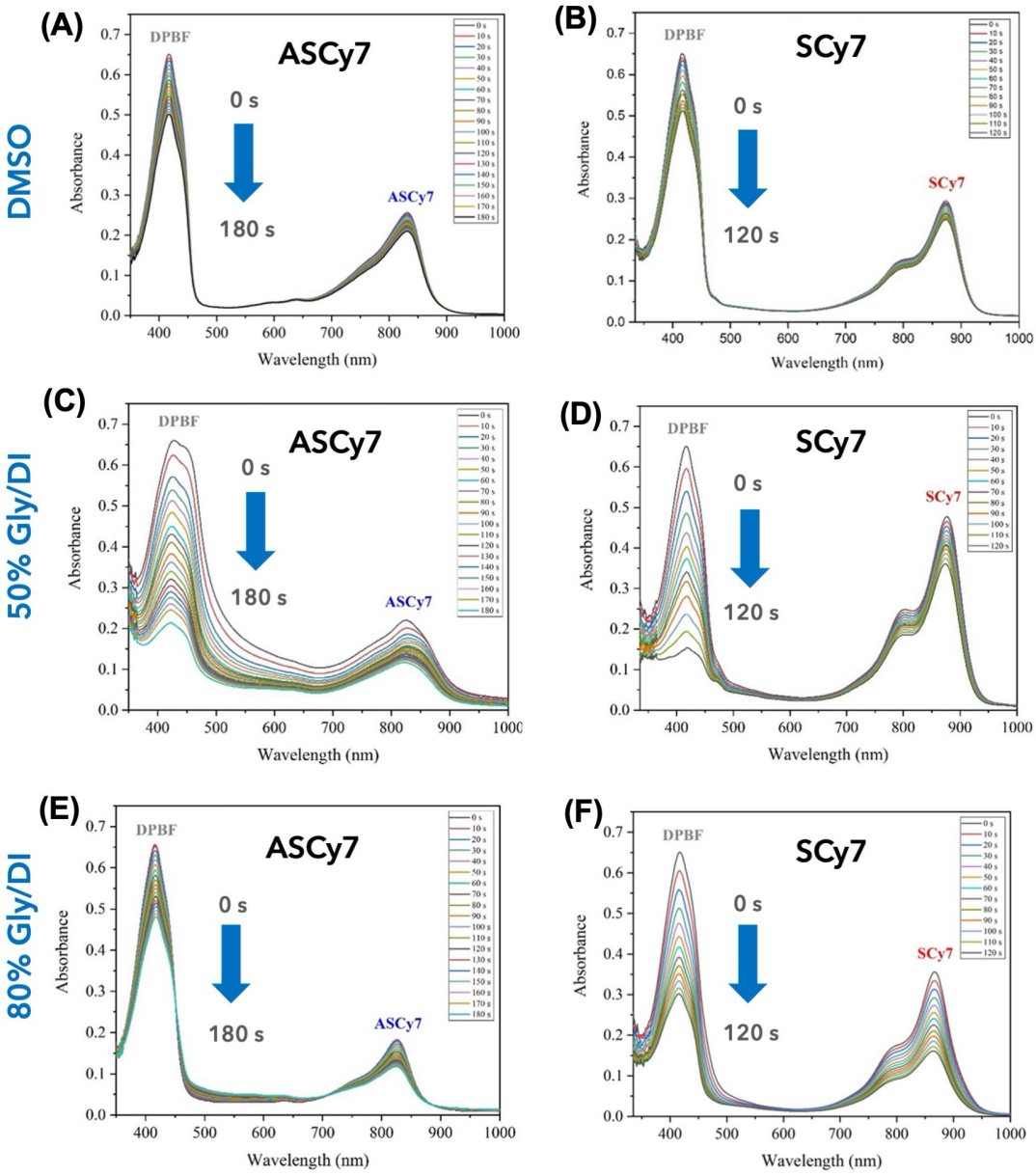

Figure S5. Singlet oxygen generation of 5 μM of (A) **ASCy7** in DMSO, (B) **SCy7** in DMSO, (C) **ASCy7** in 50% Glycerol/DI, (D) **SCy7** in 50% Glycerol/DI, (E) **ASCy7** in 80% Glycerol/DI, and (F) **SCy7** in 80% Glycerol/DI

6.2. DPBF-based assay of ICG

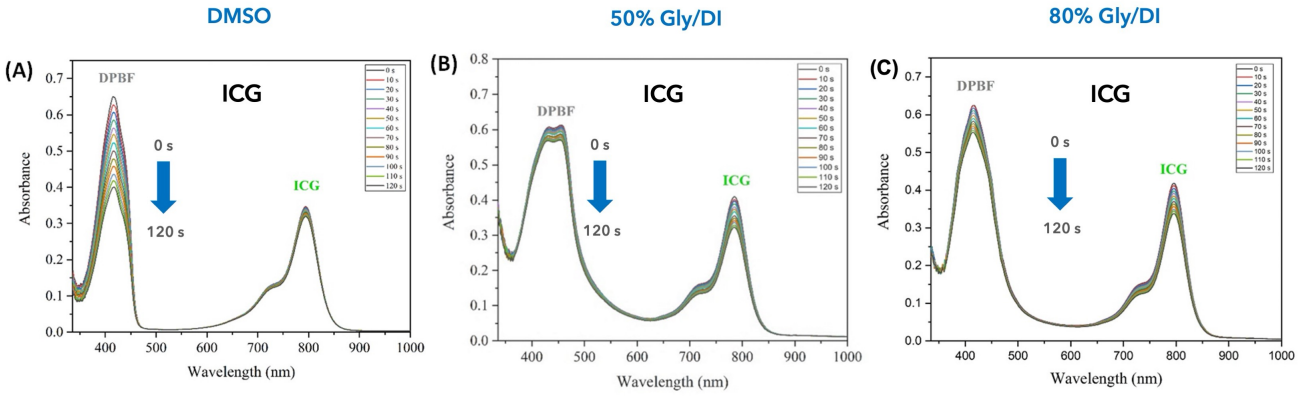

Figure S6. Singlet oxygen generation of 5 μM of ICG in (A) DMSO, (B) 50% Glycerol/DI, and (C) 80% Glycerol/DI.

6.3. Linear fitting curves of DPBF-based assay of ASCy7, SCY7 and ICG under different viscosity conditions

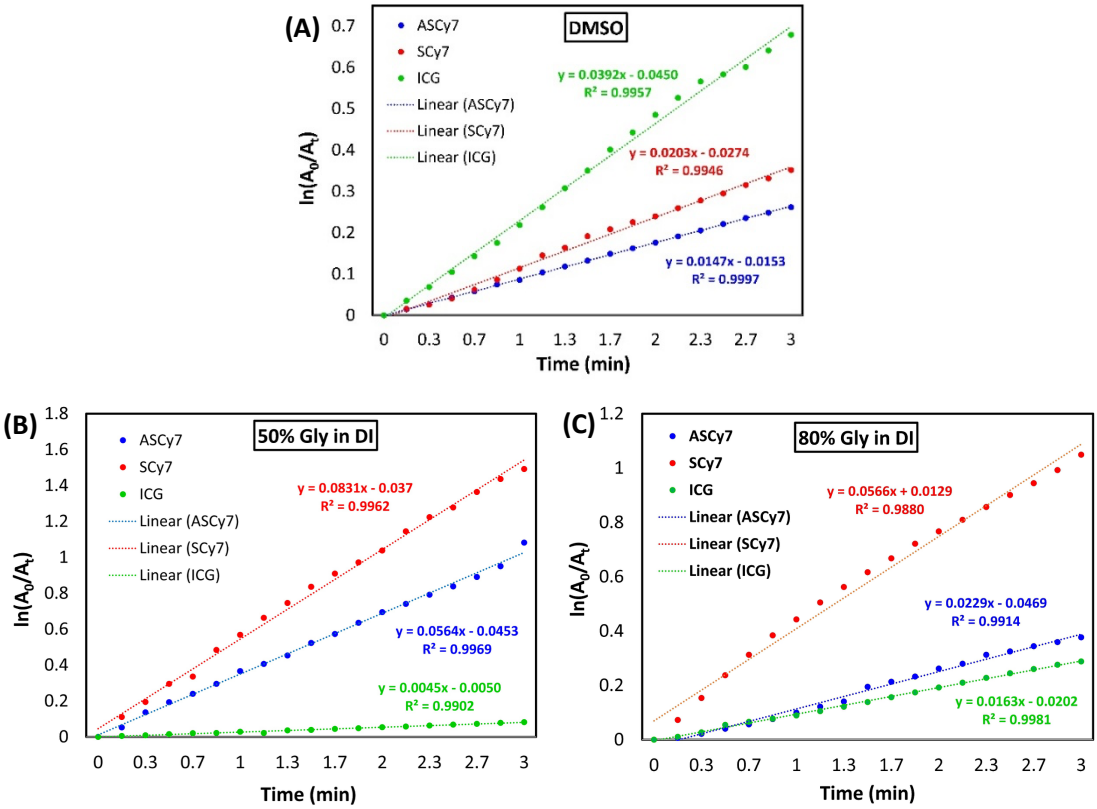

Figure S7. Linear fitting curves comparing the DPBF-based singlet oxygen generation rates of **ASCy7**, **SCy7**, and ICG in (A) DMSO, (B) 50% Glycerol/DI, and (C) 80% Glycerol/DI.

6.4. SOSG-based assay of ASCy7 and SCy7

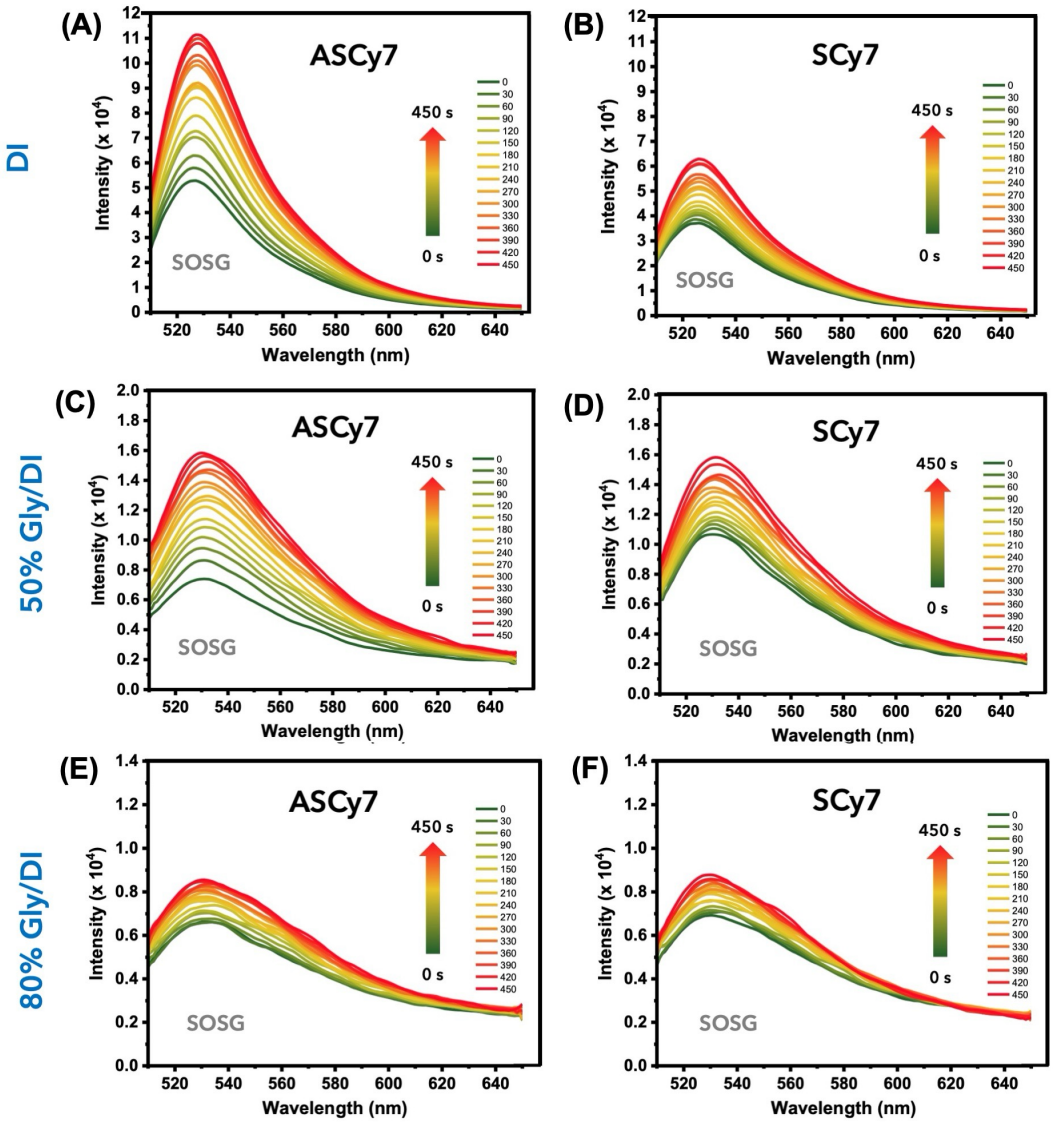

Figure S8. Singlet oxygen generation of 5 μM of (A) **ASCy7** in DI, (B) **SCy7** in DI, (C) **ASCy7** in 50% Glycerol/DI, (D) **SCy7** in 50% Glycerol/DI, (E) **ASCy7** in 80% Glycerol/DI, and (F) **SCy7** in 80% Glycerol/DI.

6.5. SOSG-based assay of ICG

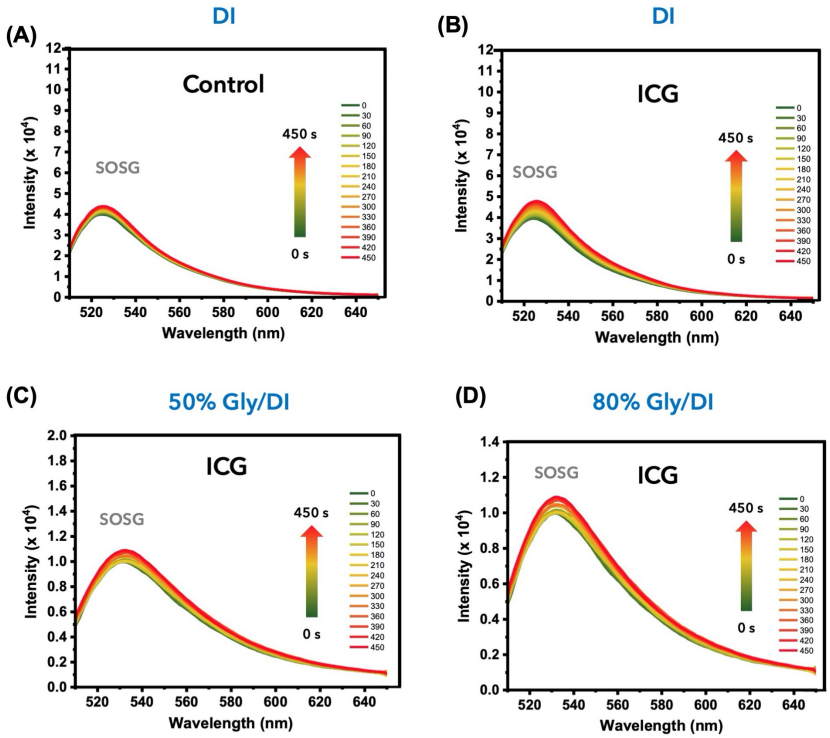

Figure S9. Singlet oxygen generation of 5 μM of (A) Control (SOSG) in DI, (B) ICG in DI, (C) ICG in 50% Glycerol/DI, and (D) ICG in 80% Glycerol/DI.

6.6. Relative curves of SOSG-based assay of ASCy7, SCY7 and ICG under different viscosity conditions

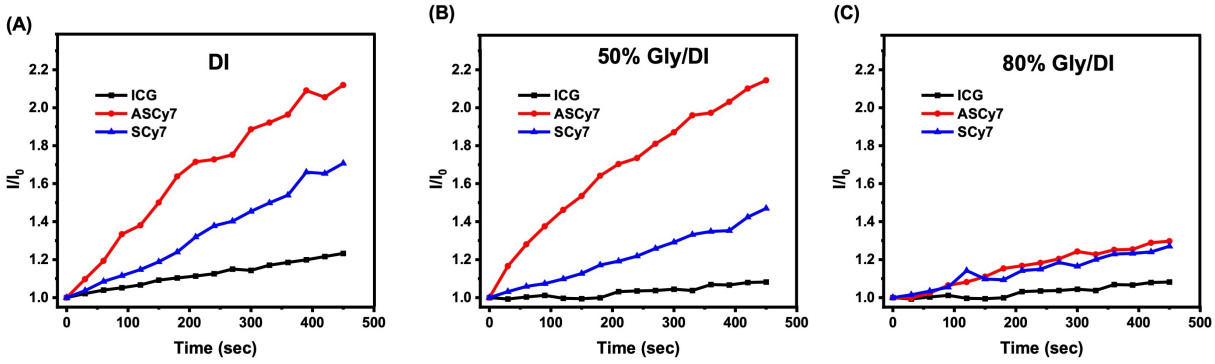

Figure S10. Linear curves comparing the SOSG-based singlet oxygen generation rates of **ASCy7**, **SCy7**, and ICG in (A) DMSO, (B) 50% Glycerol/DI, and (C) 80% Glycerol/DI.

6.7. Relative curves of DPBF-based assay of ASCy7 and SCy7 Confirmed by Singlet Oxygen Quenching using NaN_3 at 50% Glycerol/DI

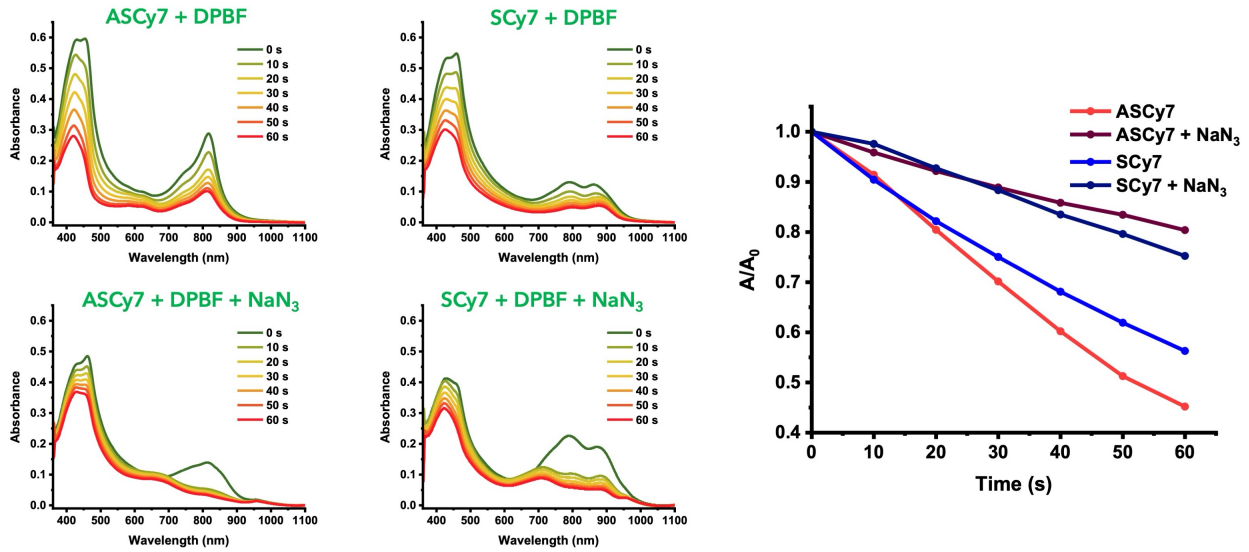

Figure S11. DPBF-based singlet oxygen detection for **ASCy7** (5 μM) and **SCy7** (5 μM) under 850 nm irradiation. Time-resolved UV–vis spectra (left) and normalized DPBF (50 μM) decay (right) demonstrate efficient $^1O_2$ generation, which is significantly suppressed by NaN_3 (10 μM), confirming a singlet oxygen–dominated photodynamic mechanism.

7. Photothermal test

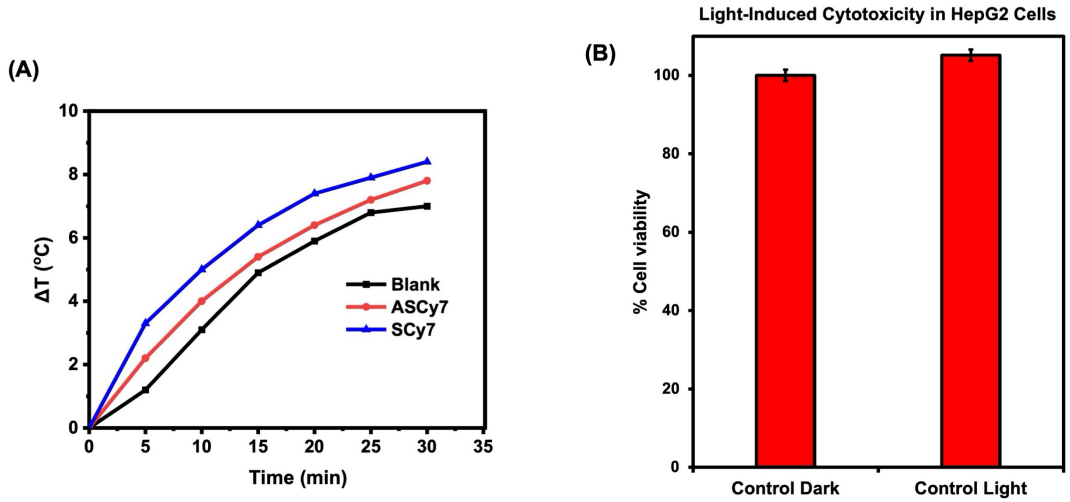

Figure S12. (A) Photothermal heating curves of **ASCy7** and **SCy7** (10 μM in PBS) under 850 nm irradiation for 0–30 min. (B) Comparison of cytotoxicity in HepG2 cells under dark conditions and 850 nm light irradiation.

8. Photostability test

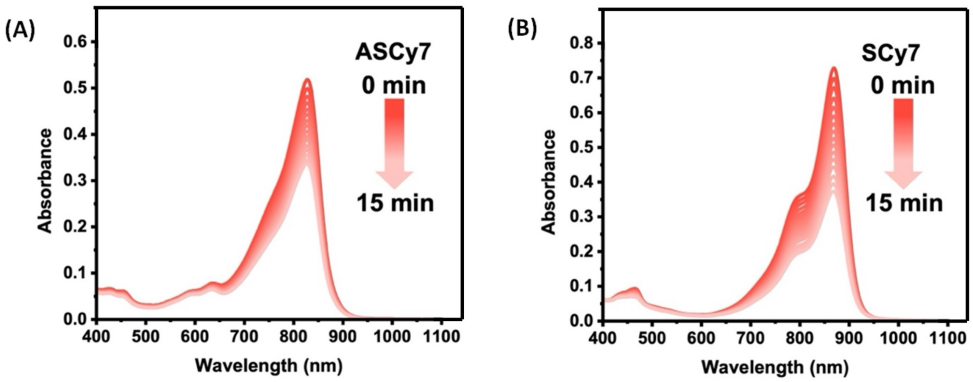

Figure S13. Photostability of (A) **ASCy7** and (B) **SCy7** under 850 nm irradiation for 0-15 min.

9. Cell internalization

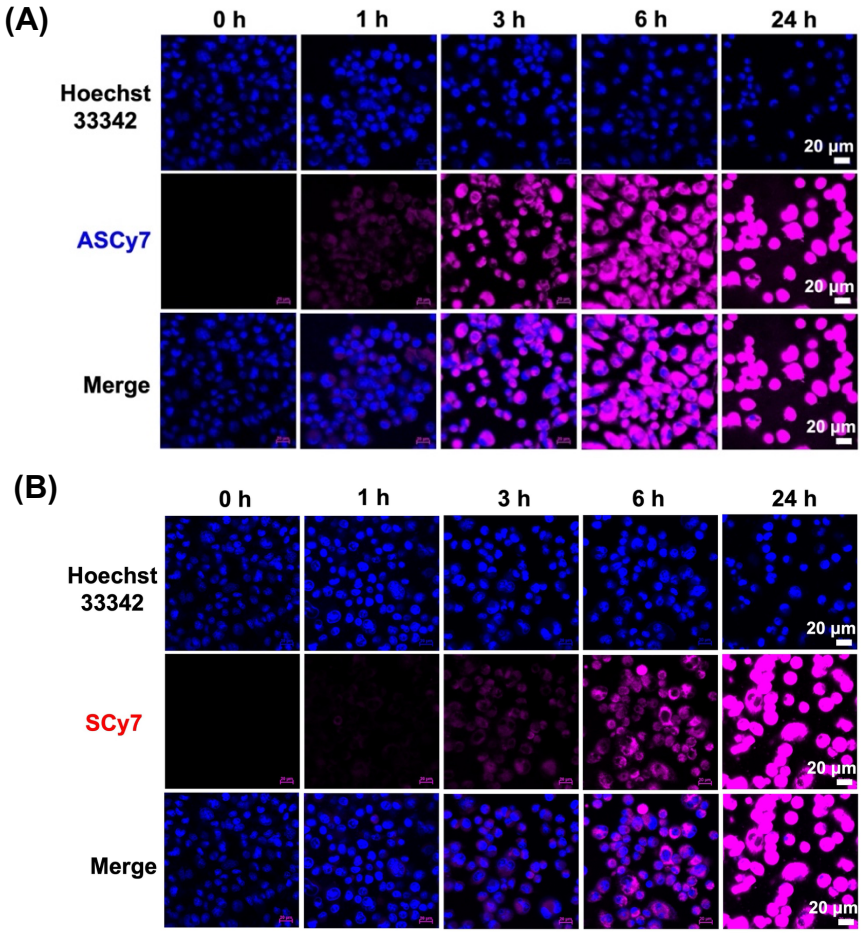

Figure S14. Confocal images of HepG2 cells incubated with 2.5 μM of (A) **ASCy7** and (B) **SCy7** for 0, 1, 3, 6, and 24 h.

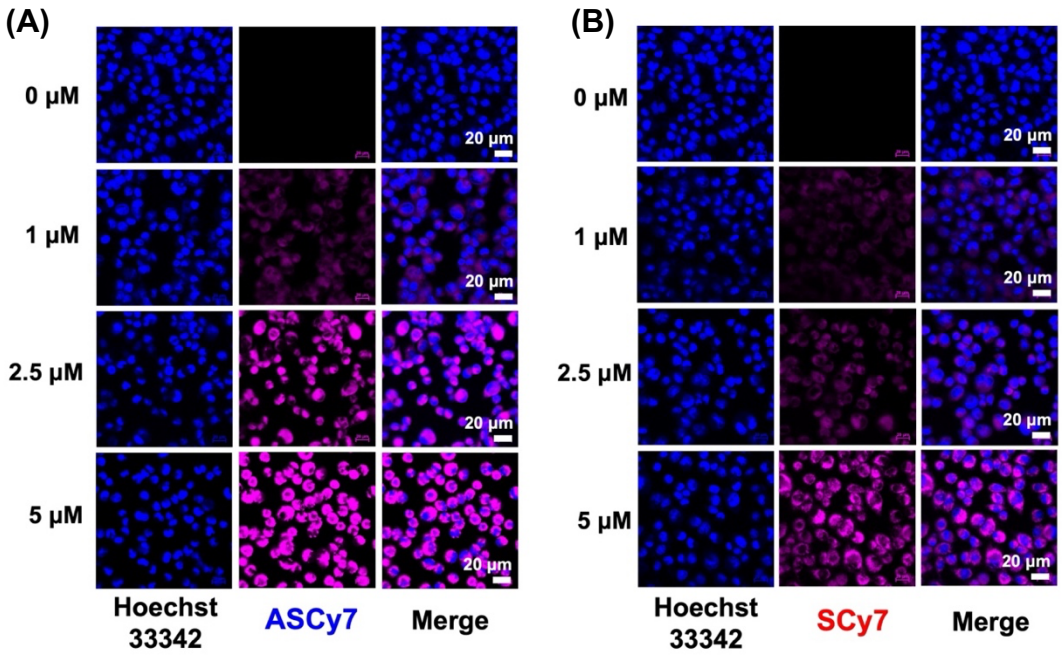

Figure S15. Confocal images of HepG2 cells were treated with (A) **ASCy7** (B) **SCy7** (0, 1, 2.5, 5 μM) for 3 h. Scale bar = 20 μm.

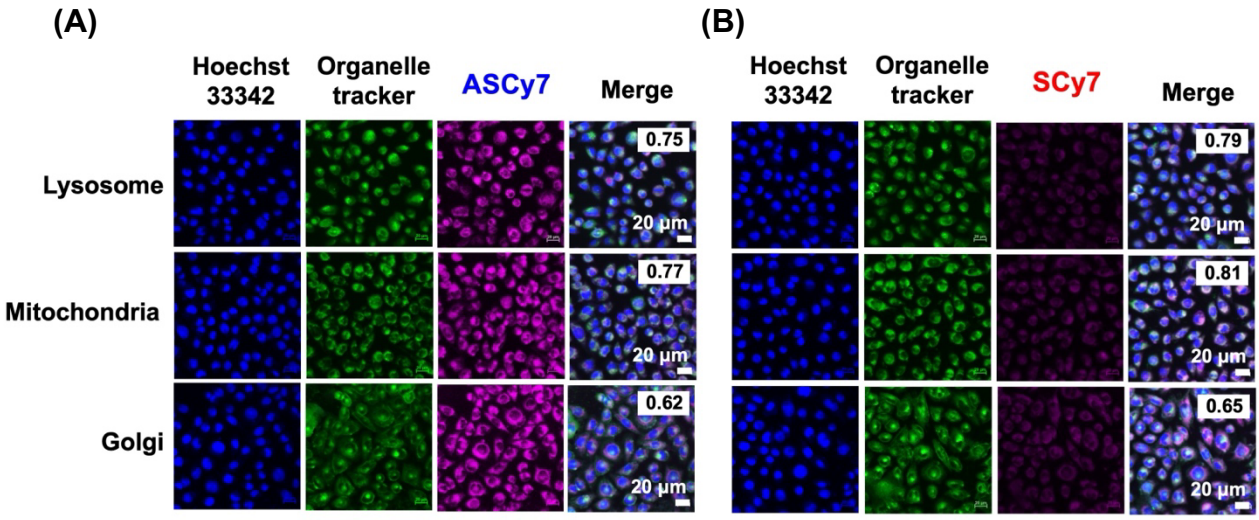

Figure S16. Confocal images of HepG2 cells incubated with 2.5 μM of (A) **ASCy7** (B) **SCy7** for 3 h and then incubated with organelle trackers: LysoTracker, MitoTracker, and NBD Ceramide (1 μM) for 10 min. Scale bar = 20 μm.

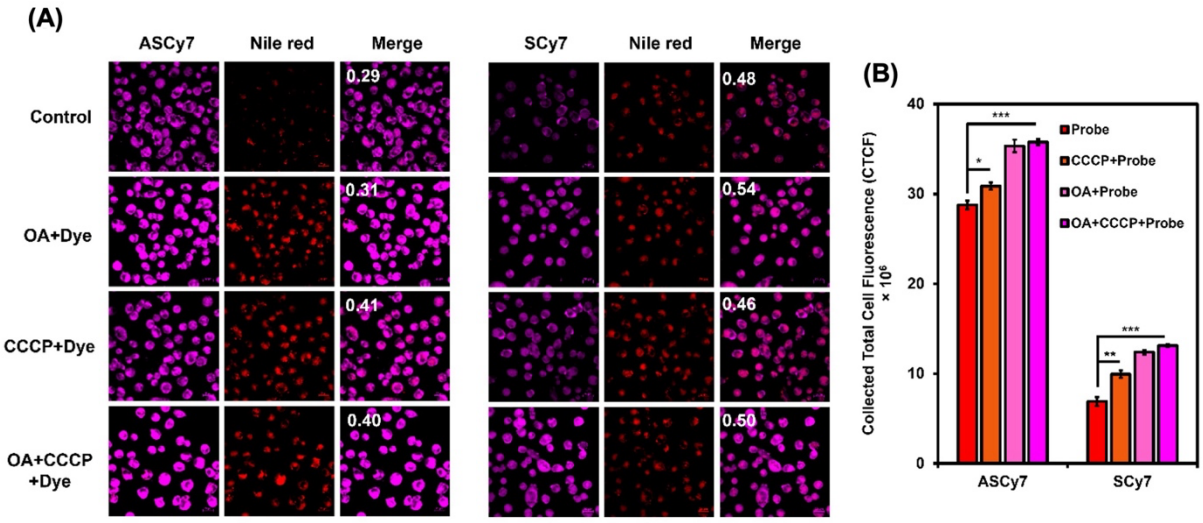

Figure S17. (A) Confocal fluorescence images showing colocalization of **ASCy7** and **SCy7** with Nile red under control and OA/CCCP-treated conditions. (B) Corresponding quantification of collected total cell fluorescence (CTCF). Mean ± SD (n = 30); ***$P < 0.001$ by one-way ANOVA (Tukey). Scale bars = 20 μm.

10. Cytotoxicity assays

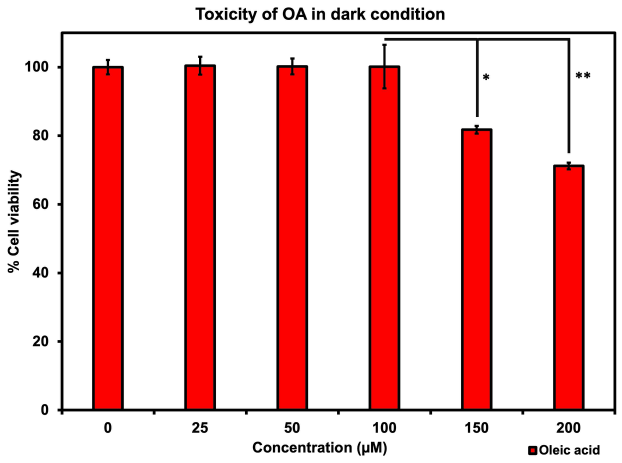

Figure S18. Dark toxicity of oleic acid at different concentrations.

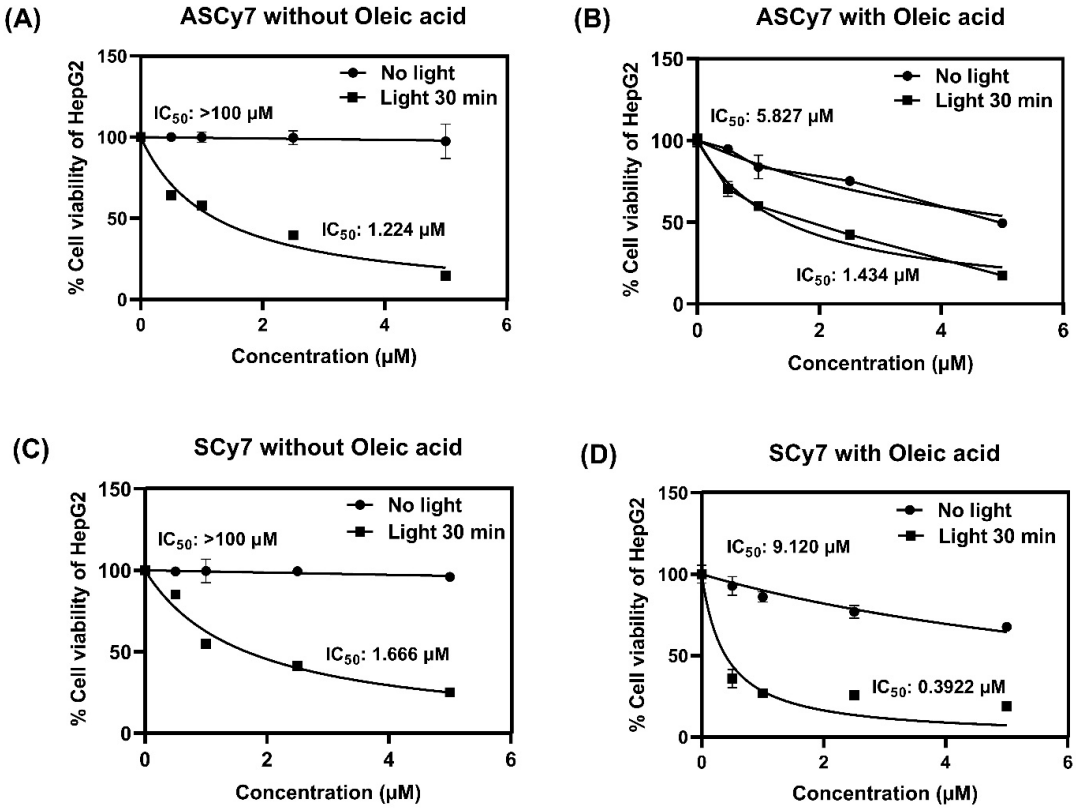

Figure S19. IC_{50} curves of (A) **ASCy7** without Oleic acid, (B) **ASCy7** with Oleic acid, (C) **SCy7** without Oleic acid, (D) **SCy7** with Oleic acid for HepG2.

11. ^{1}H and ^{13}C NMR spectra of ASCy7

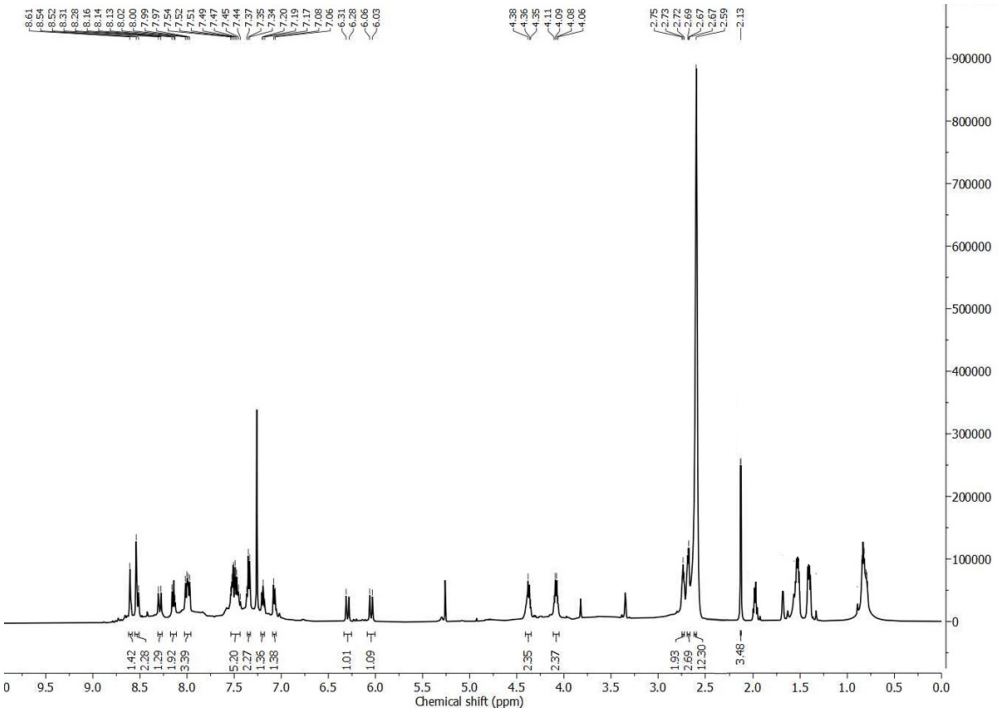

Fig. S20. ^{1}H NMR of **ASCy7** in chloroform-*d*

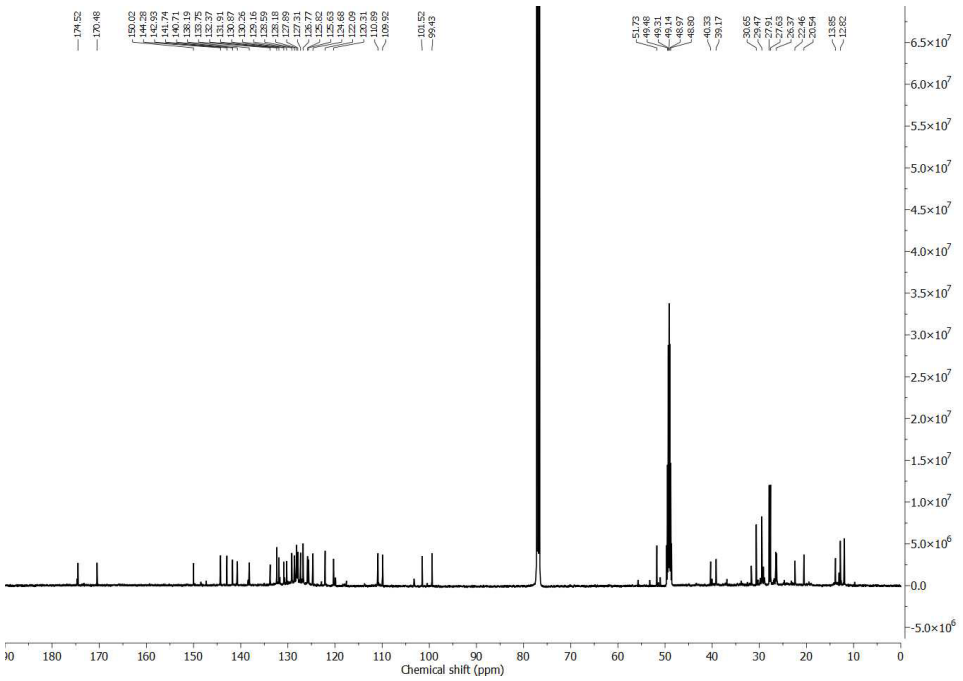

Fig. S21. ^{13}C NMR of **ASCy7** in chloroform-*d*

12. ^{1}H and ^{13}C NMR spectra of SCy7

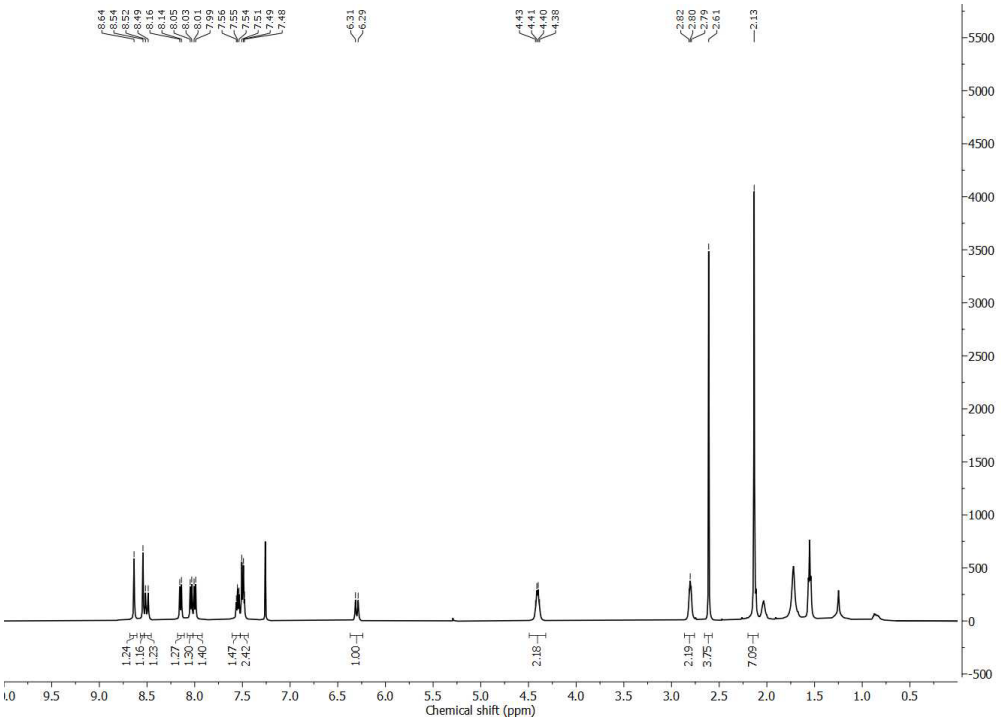

Fig. S22. ^{1}H NMR of **SCy7** in chloroform-*d*

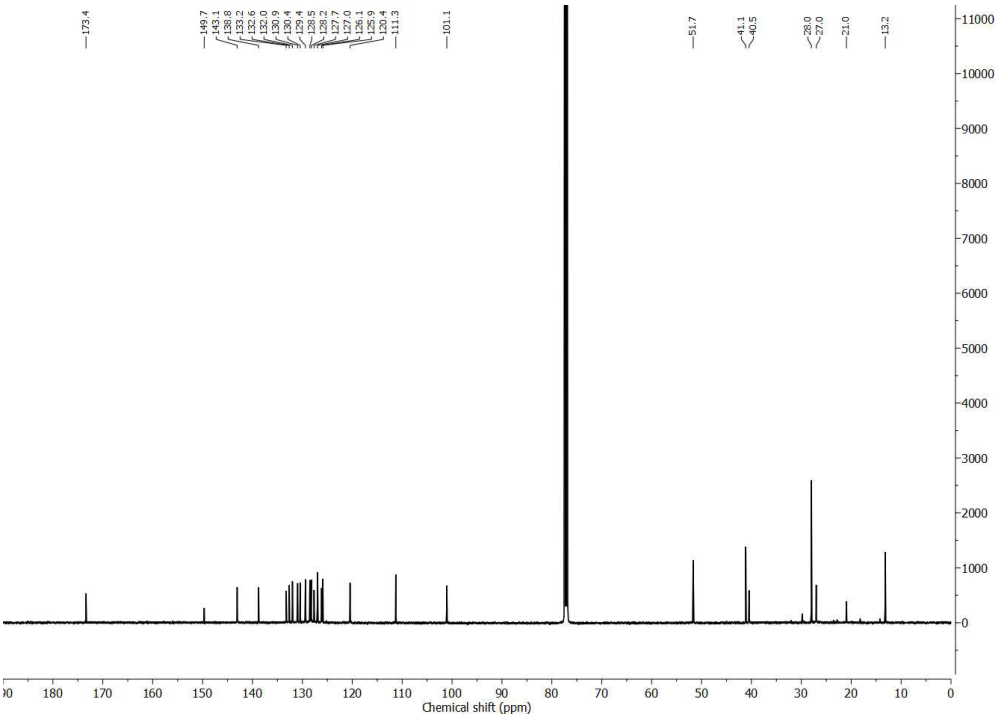

Fig. S23. ^{13}C NMR of **SCy7** in chloroform-*d*

13. Mass spectrum of ASCy7 and SCy7

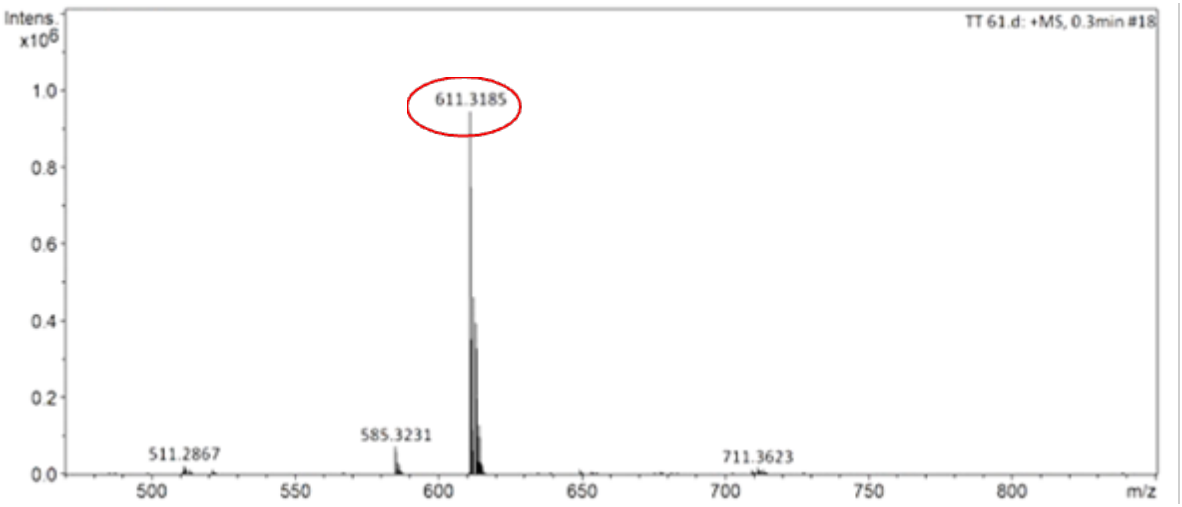

Fig. S24. HRMS spectrum of **ASCy7**

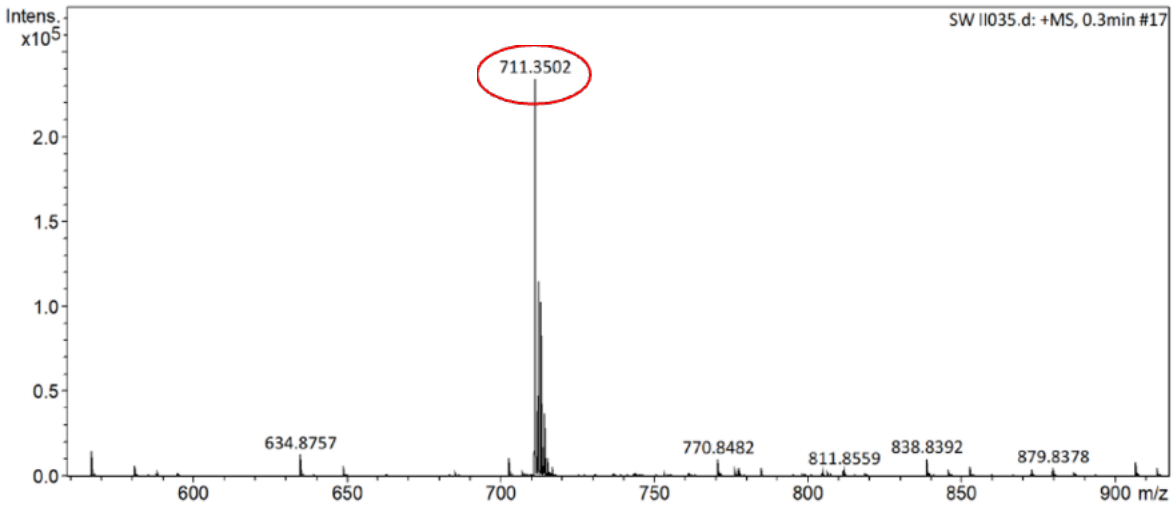

Fig. S25. HRMS spectrum of **SCy7**